Journal of Hydrology: Regional Studies 42 (2022) 101177

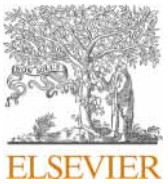

Contents lists available at ScienceDirect

Journal of Hydrology: Regional Studies

journal homepage: www.elsevier.com/locate/ejrh

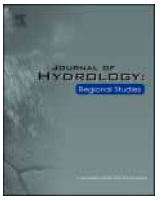

# When climate variability partly compensates for groundwater depletion: An analysis of the GRACE signal in Morocco

Hamza Ouatiki [a,b,*], Abdelghani Boudhar [a,b], Marc Leblanc [c,d,e], Younes Fakir [a,f], Abdelghani Chehbouni [a,c]

[a] Center for Remote Sensing Applications (CRSA), Mohammed VI Polytechnic University, Ben Guerir 43150, Morocco
[b] Data4Earth Laboratory, Sultan Moulay Slimane University, Beni Mellal 23000, Morocco
[c] International Water Research Institute (IWRI), Mohammed VI Polytechnic University, Ben Guerir 43150, Morocco
[d] Hydrogeology Laboratory, UMR EMMAH, University of Avignon, Avignon 84000, France
[e] UMR G-EAU, IRD, Montpellier 34090, France
[f] Department of Geology, Faculty of Sciences–Semlalia, Cadi Ayyad University, Marrakech 40001, Morocco

ARTICLE INFO

*Keywords:*
GRACE
Groundwater depletion
Changepoint
Natural recharge
GRACE versus climate

ABSTRACT

*Study region:* Morocco, Northwestern Africa.
*Study focus:* Since April 2002, the Gravity Recovery and Climate Experiment (GRACE) mission have opened new pathways for hydrologists to monitor the changes in terrestrial total water storage (TWS). Here, the Center for Space Research (CSR), Goddard Space Flight Center (GSFC), Jet Propulsion Laboratory (JPL), and the average (AVG) GRACE mascon solutions were used to examine the changes in TWS and groundwater storages (GWS) in Morocco, with an emphasis on natural replenishment events and their link to snow cover area (SCA) and rainfall variability.
*New hydrological insights for the region:* The results showed that GRACE TWS from AVG ($TWS_{AVG}$) and GSFC ($TWS_{GSFC}$) can fairly describe the temporal patterns of the groundwater level (GWL). Moreover, during 2002–2020, the TWS underwent a strong depletion relatively masked by natural recharge events. This was revealed as we identified two intermittent depletion episodes with statistically significant rates ($-1.03 \pm 0.11$ to $-0.31 \pm 0.1$ cm $yr^{-1}$) higher than those obtained for the long-term trend lines ($-0.28 \pm 0.11$ to $-0.15 \pm 0.07$ cm $yr^{-1}$). The TWS appeared to be strongly linked with the SCA metrics and rainfall indices with 1–3 months of lag. Our findings suggest that the rainfall distribution can be more insightful about changes in groundwater levels compared to the rainfall monthly totals.

## 1. Introduction

Surface water is often considered as the primary source intended to satisfy the demand of different sectors. In Agriculture, one of the main water consumers in Morocco, crop irrigation from dam allocations and rainfall are preferable given their cost-effective use compared to groundwater. However, the decreasing tendencies in rainfall totals combined with the irregular distribution of event occurrence in recent decades (Filahi et al., 2015; IPCC, 2014; Ouatiki et al., 2019) have led to more reliance on groundwater. Population growth in its turn escalated this reliance as more wells were drilled to meet the growing water demand for domestic usage

* Corresponding author at: Center for Remote Sensing Applications (CRSA), Mohammed VI Polytechnic University, Ben Guerir 43150, Morocco.
*E-mail address:* hamza.ouatiki@um6p.ma (H. Ouatiki).

https://doi.org/10.1016/j.ejrh.2022.101177
Received 23 February 2022; Received in revised form 12 July 2022; Accepted 14 July 2022
Available online 19 July 2022

(Bouchaou et al., 2009). Thus, an increase in pumping has provoked a serious depletion in the water table since the 1990 s. Drops of 5–65 m in the groundwater level were registered between 1990 and 2019 in various regions in Morocco (Bahir et al., 2021; Hssaisoune et al., 2020; Ouassanouan et al., 2022). This situation is more likely to worsen as future scenarios suggest further decline and irregularity in surface water supplies (Filahi et al., 2017; Marchane et al., 2021). Nevertheless, the long-term depletion is often palliated by continuous yet low natural recharge. The latter is mainly ensured by surface water infiltration through river beds, irrigation, and precipitation received over the lowlands and the mountainous regions (Bouchaou et al., 2009; Bouimouass et al., 2020; Fakir et al., 2021). Still, the imbalance between the extraction and natural recharge rates makes it difficult to reach sustainability (Hssaisoune et al., 2020).

In view of the above-mentioned challenges, understanding the variability of groundwater storage is essential for sustainable management and optimal planning of water resources. This is critical information for planning socio-economic development and environmental sustainability, especially in countries with a GDP highly dependent on agricultural yields, such as Morocco. Despite the major role groundwater resources play on many levels, their monitoring remains inconsistent and limited in both temporal and spatial scales. The shortage in piezometers and controlled wells, and thus the lack of relevant and temporally continuous observations are the main limiting factors. Remote sensing observations collected by multiple satellite-based sensors offer a promising venue to complement in situ data. Various spatial missions freely provide global and gridded estimates of different components of the hydrologic cycle. Recent advances have been made in snow cover (Hall and Riggs, 2016) and soil moisture retrievals (Entekhabi et al., 2010) employing data from optical and microwave sensors. The equivalent water thickness of these water cycle components in addition to groundwater are summed up by the GRACE and its follow-on (GRACE-FO) mission in what so-called total water storage anomalies (Tapley et al., 2019). The mission, jointly launched by NASA and German (DLR) space agencies, acquire changes in gravity fields. The latter are generally driven by water mass redistribution on top and beneath the earth's surface. This opened huge opportunities for studying the water stored in reservoirs and land-atmosphere fluxes (Eicker et al., 2020).

In the last two decades, GRACE was considered in various water-related applications (Asoka et al., 2017; Döll et al., 2014; Ferreira et al., 2020; Xiao et al., 2015). Many studies have investigated its robustness against the groundwater level observations. The water storage estimates were found to agree very well with the in-situ measurements in different regions worldwide, particularly the mascon solutions showed the best match (Bhanja et al., 2018; Neves et al., 2020; Shen et al., 2015; Xie et al., 2018). Noteworthy, good agreement was also reported for groundwater storage determined using spherical harmonic solutions (Ferreira et al., 2020).

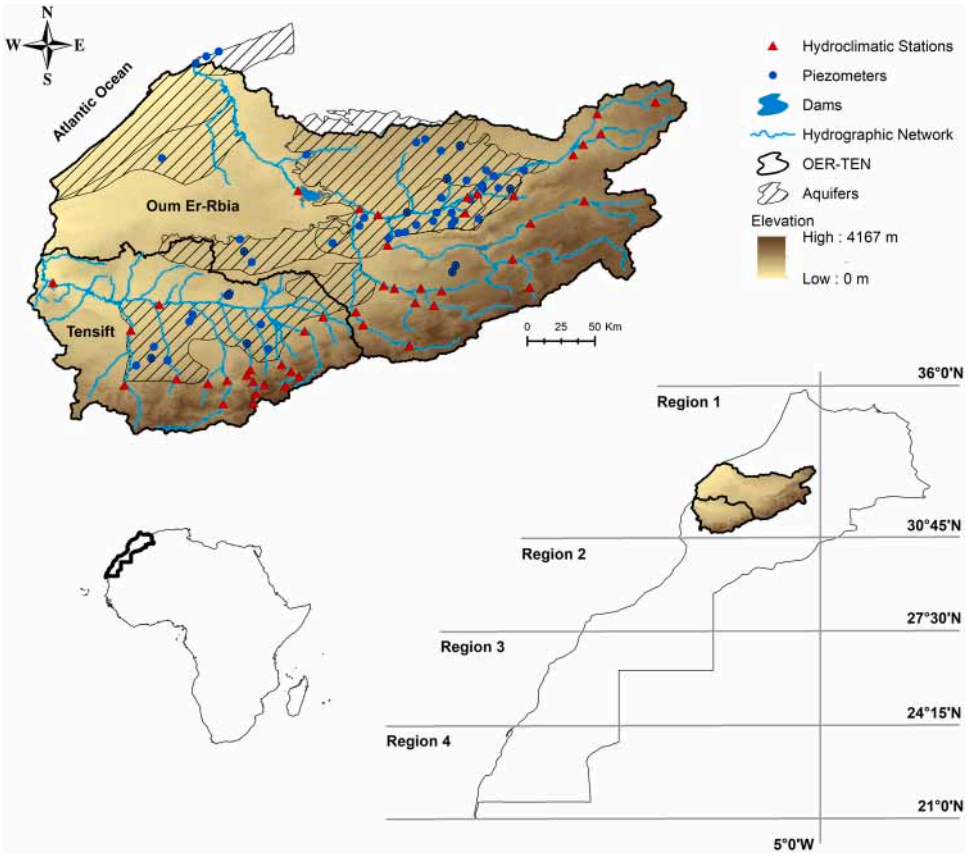


**Fig. 1.** Key features of the Oum Er-Rbia and Tensift river basins. The piezometers identified with a black dot in the center are the ones used in the present study.

Additionally, the GRACE data were combined with outputs from hydrologic and land surface models to strengthen the accuracy of the water balance estimation (Gleason et al., 2018; Mehrnegar et al., 2020). They have proved adequate to improve surface soil moisture estimation over densely vegetated areas (where the passive microwave estimates are susceptible to uncertainties) and evapotranspiration mapping in water-limited regions (Sadeghi et al., 2020; Shen et al., 2017). GRACE was used to map the ice mass loss estimates over glaciers (Doumbia et al., 2020; Jin et al., 2017), and quantify snow accumulation over high-latitudes adopting a mass balance approach (Behrangi et al., 2018; Niu et al., 2007). More frequently, the GRACE time series were used to analyze the long-term temporal changes in groundwater storage and its susceptibility to climate variability (Ahmed, 2020; Ahmed et al., 2014; Bhanja et al., 2018; Hasan et al., 2019; Leblanc et al., 2011, 2009; Shen et al., 2015; Xie et al., 2018). In Morocco, two studies explored the patterns of groundwater using GRACE measurements (Ahmed et al., 2021; Milewski et al., 2020). The authors compared the trend lines' slopes of rainfall and GRACE-based groundwater anomalies to explain the sustainability of the groundwater resources. In this study, we aim at assessing the temporal variability of terrestrial water storage over Morocco, with an emphasis on its link to rainfall and snow cover patterns. Based on trend test and correlation analysis, we shed light on the interaction between climate variability and terrestrial water storage, and how surface water intakes can relatively mask the ongoing depletion.

## 2. Methods

### 2.1. Study area

The study covers Morocco in northwestern Africa. It was firstly held over the whole territory subdivided into four subregions (Region 1–4) and then focused on an area of smaller scale (Fig. 1). The latter include the Oum Er-Rbia (OER) and Tensift (TEN) river basins grouped together (OER-TEN hereafter), occupying a surface of approximately 64 000 km$^2$. The region is bordered from the east by the Atlas mountain chain (culminating at 4124 m a.s.l.) that holds the credit for most of the water supplying the surrounding lowlands (Boudhar et al., 2011; Ouatiki et al., 2020). The water stored in aquifers (deep confined and shallow unconfined) and dams support the allocation for drinking, industrial and agricultural activities (325 800 ha of irrigated lands), and electricity production through hydropower plants. The OER-TEN is mainly influenced by the North Atlantic oscillation (Knippertz et al., 2003). It is dominated by semi-arid conditions that become relatively humid as we move towards high elevations. The rainfall is strongly variable over space and time (Hadri et al., 2021; Ouatiki et al., 2019). Its annual cycle is characterized by a wet period from November to April and a dry period from Jun to September with the highest and lowest totals usually recorded during the winter (December, January, and February) and summer months (June, July, and August), respectively. Above 1000 m a.s.l., precipitation occurs as snow between mid-November and mid-April and completely vanishes during the hot summer (Boudhar et al., 2020, 2016).

### 2.2. Rainfall

Daily rainfall records from ground rain gauges situated within the OER and TEN river basins were used in this study. With a temporal coverage of 39 hydrologic years (09/1976–08/2015) the data were provided by the Oum Er-Rbia and Tensift Hydraulic Agencies (ABHOER and ABHT, respectively), and the Regional Office for Agricultural Development of Tadla (ORMVAT). The daily observations were processed to calculate four rainfall indices at monthly and annual time scales, according to the Climate Change Indices list provided by the Expert Team on Climate Change Detection and Indices (Peterson et al., 2001):

1) Rainfall: the total rainfall (in mm) per month/year.
2) NWD: the count (in days) of wet days per month/year. A day is considered as wet when the total rainfall exceeds a certain threshold. In the present study, six different thresholds (0.1 mm, 1 mm, 2 mm, 3 mm, 4 mm, and 5 mm) were tested to define a wet day.
3) NCWD: the count (in days) of wet spells with at least 2 consecutive wet days.
4) MCWD: The length (in days) of the wet spells exhibiting the maximum consecutive wet days.

In addition to the in-situ observations, gridded satellite rainfall estimates from the Precipitation Estimation from Remotely Sensed Information Using Artificial Neural Networks - Climate Data Record (PERSIANN-CDR) product were employed (Ashouri et al., 2015). The final PERSIANN-CDR data is provided as quasi-global (60°S to 60°N) rainfall estimates at 0.25°x 0.25° spatial resolution every 3 h. The product was chosen considering the good performance it showed when evaluated against rain gauges within the study region (Ouatiki et al., 2022 in review). Although slightly surpassed by the Integrated Multi-satellitE Retrievals for GPM (IMERG), PERSIANN-CDR was preferred given its availability for a period (from 1983 to the present) long enough to allow relevant climatological analysis. We must highlight that the term year, hereafter, refers to the hydrologic year (from September to August, e.g., 01/09/2002–31/08/2003, 2002/2003).

### 2.3. Snow cover area

Snow depth measurement stations are relatively scarce over the OER-TEN's mountainous region (20 000 km$^2$ above 1000 m a.s.l.). Thus, SCA retrieved from Terra MODIS satellite data (MOD10A1) is used in this study as an alternative for snow in situ measurements (Hall and Riggs, 2016). MOD10A1 product provides daily observations spatially gridded at 500 m from 2000 to the present. Moreover, to deal with the missing values and cloud coverage effect, the SCA daily maps were processed adopting a method developed for the Moroccan Atlas mountain range (Marchane et al., 2015). Using the corrected MOD10A1 data, time series of snow cover area in

percentage (SCAp) were built relative to the total area of the OER-TEN's mountainous region. Thus, three metrics (maximum, median, and average) of the daily SCAp were derived for each month and year of the period 2000–2015.

### 2.4. Soil moisture

The soil moisture (SM) estimates were obtained at 100 cm depth via the SURFEX (in french Surface Externalisée) surface modeling platform developed by Météo-France (Albergel et al., 2019). The platform includes the ISBA land surface model implemented with the TRIP (Oki and Sud, 1998) hydrologic model through a global land data assimilation system (LDAS-Monde)(Albergel et al., 2017). The latter permits the incorporation of surface soil moisture (SM) and leaf area index satellite observations to constrain the near-surface variables (including SM) simulated by the ISBA-TRIP coupled model. More information can be found on SURFEX official website (http://www.umr-cnrm.fr/surfex/, last access: August 2021).

### 2.5. Groundwater level

GWL from 44 piezometers were delivered by the ABHOER and ABHT. After the data quality control, 10 piezometer records that present the least amount of missing data were selected. The best temporal overlap that allowed to maximize the number of retained piezometers was found for the period 2002–2017. The available piezometers are distributed over the whole study region and capture the majority of the aquifers. Average monthly GWL time series were calculated for OER-TEN. In this study, given the lack of specific yield estimates in addition to the strong heterogeneity of the aquifer systems over the study region, we did not consider the groundwater storage from in-situ observations. Instead, we have standardized the groundwater level time series of each well by subtracting the mean and dividing by the standard deviation before computing the regional groundwater level average (Bloomfield and Marchant, 2013; Zhao et al., 2017). This approach adopted by Ahmed et al. (2021) over the same context, can maintain information about the temporal patterns (the main focus here) of the groundwater level.

### 2.6. Surface water bodies

In the OER-TEN basin, surface water is mostly represented through anthropogenic hydraulic infrastructures. These facilities are jointly managed and regulated by the ABHOER and the National Office of Electricity and Drinking Water (ONEE) to support the water needs for drinking and socioeconomic activities. The monthly storage time series of the two largest dams (Bin El Ouidane and Al Massira) were considered in this study to account for the surface water effect on GRACE TWS estimates. The data were obtained from the ABHOER for the period between 2002 and 2017.

### 2.7. GRACE mission

GRACE (April 2002–June 2017) and GRACE-FO (June 2018–present), jointly launched by NASA and DLR, map the Earth's monthly gravity changes provoked by mass redistribution above and below the earth's surface (Tapley et al., 2019, 2004). Their end-user data are provided as equivalent water thickness anomalies and corrected for most geophysical distortions. They are available as solutions from various centers (CSR, German Research Centre for Geosciences (GFZ), JPL, and GSFC) in spherical harmonics and/or mascons (mass concentration blocks) versions. The mascons are newly released as an alternative for solving the gravity signals and have advantages over spherical harmonics. They are less subject to leakage errors and show better land-ocean signals separation (Landerer and Cooley, 2021; Luthcke et al., 2013; Watkins et al., 2015). Several studies indicated the precedence of mascon solutions over the harmonic in representing the groundwater variations (Bhanja et al., 2018, 2016; Neves et al., 2020; Xie et al., 2018).

The earth's monthly terrestrial TWS anomalies from JPL, CSR, and GSFC GRACE mascon solutions were used in this work for the period 2002–2020. The data are available at different spatial samplings with a native resolution of about 3°x3°. The three solutions were averaged to obtain a mean TWS time series. The errors associated with the average TWS were computed as the monthly standard deviation of the three solutions (Ahmed and Wiese, 2019). Due to measures taken for battery saving, the TWS time series contain some missing months. The latter were filled by using a three-month moving average window. However, when more than two successive months were missing, the gaps were omitted during all of the analyses considered in this study. The TWS sums the water masses contained in the different terrestrial reservoirs: Surface Water Bodies (SWB), Snow Water Equivalent (SWE), SM, GWS, Canopy (Ca) (Shen et al., 2015). Employing the mass balance approach, the changes in the GWS can be estimated as:

$$\mathrm{GWS} = \mathrm{TWS} - (\mathrm{SWB} + \mathrm{SWE} + \mathrm{SM} + \mathrm{Ca}) \quad (1)$$

One or more of the equation terms (SWB, SWE, SM, or Ca) can be omitted according to their significance to the long-term variations in the TWS (Shen et al., 2015). Here the GWS was derived from the TWS based on SWB, and SM. The errors associated with the GWS data were computed as the root sum of squares of the errors associated with each of the terms considered in the GWS estimation (Eq. (2)).

$$\sigma_{\mathrm{GWS}} = \sqrt{\sigma_{\mathrm{TWS}} + \sigma_{\mathrm{SM}} + \sigma_{\mathrm{SWB}}} \quad (2)$$

Where $\sigma_{\mathrm{GWS}}$ is the error in GRACE-based GWS, $\sigma_{\mathrm{TWS}}$ GRACE TWS error, $\sigma_{\mathrm{SM}}$ monthly standard deviation from SURFEX soil moistures estimates, and $\sigma_{SWB}$ is the monthly standard deviation from surface water reservoirs.

### 2.8. Statistical indices and metrics

The TWS and GWS time series were tested for monotonic trends using the seasonal Mann-Kendall test (Kendall, 1938; Mann, 1945). The magnitude of the trend was quantified based on the Theil-Sen slope estimator (Sen, 1968; Theil, 1950). To consider the impact of data inhomogeneity on the estimated trend slopes, a predefined function was used to detect the presence of potential change points in the TWS time series. The function relies on the work done by Lavielle (2005) and Killick et al. (2012) to identify the location where the mean and slope of the time series significantly change. It consecutively divides the time series into two sections and computes an estimate of the mean of each section. The change point is identified at the location where deviation of the sum of the residual error reaches a minimum value.

The Spearman rank (SCC, Eq. (3)) correlation coefficient and Root Mean Square Error (RMSE, Eq. (4)) were used to examine how well GRACE data follow the temporal patterns of the GWL observations. The SCC was also adopted to assess the linear relationship of GRACE versus the SCA metrics and rainfall indices. All the variables considered in this analysis were standardized the same way as for the GWL (Section ↱2.5). Also, a smoothing filter was applied to the GWL, SCA metrics, and rainfall indices using the Savitzky-Golay filter.

$$\mathrm{SCC} = \frac{\sum_{i=i}^{n}(R(x_i) - \overline{R(x)})(R(y_i) - \overline{R(y)})}{\sqrt{\sum_{i=1}^{n}(R(x_i) - \overline{R(x)})^2 \sum_{i=1}^{n}(R(y_i) - \overline{R(y)})^2}} \tag{3}$$

$$RMSE = \sqrt{\frac{\sum_{i=1}^{n}(x_i - y_i)^2}{n}} \tag{4}$$

where $x_i$ and $y_i$ are the values of x-variable and y-variable in the time i, respectively. $R(x_i)$ and $R(y_i)$ are the rank of the x-variable and y-variable values, respectively, with mean values of $\overline{R(x)}$ and $\overline{R(y)}$. n is the number of records.

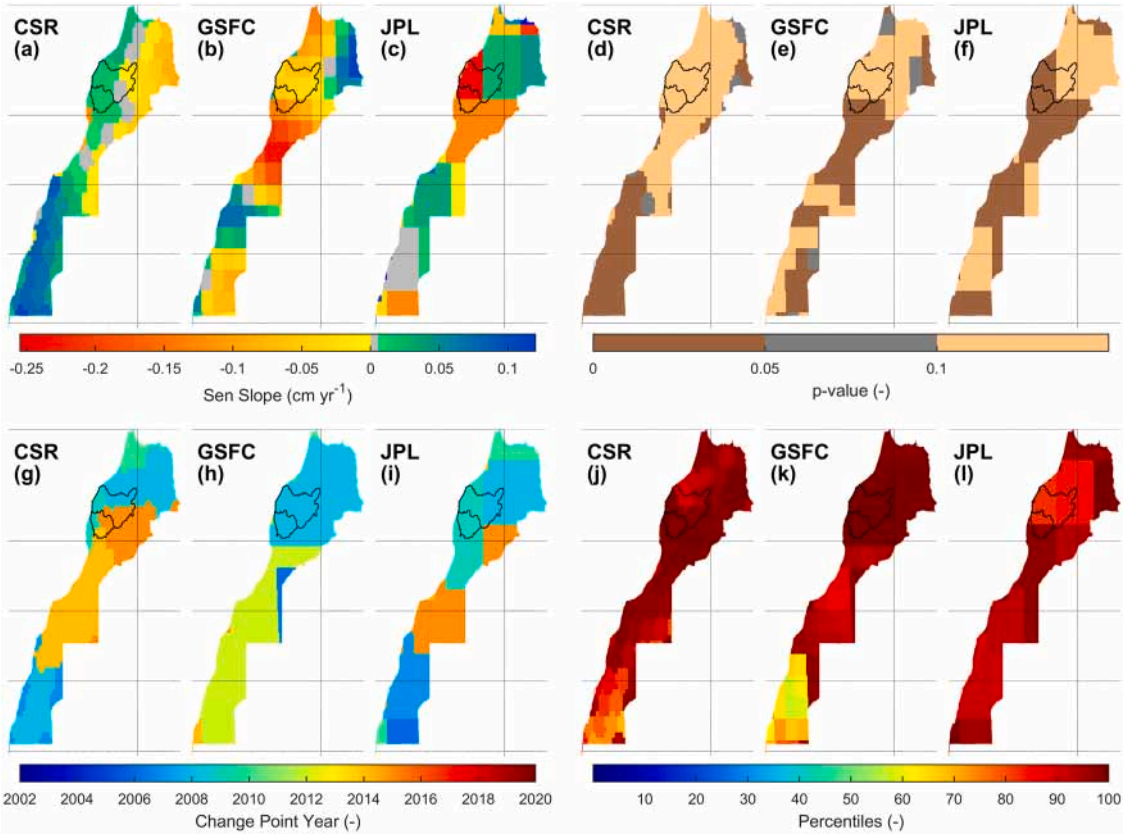


**Fig. 2.** Changes in TWS from CSR, GSFC, and JPL GRACE solutions for the period 2002 – 2020. (a)–(c): Trend magnitudes estimated using the Theil-Sen slope estimator. (d)–(f): The p-value showing the significance of the detected trends. (g)–(i): The years where significant changes have occurred in the mean and slope of the TWS monthly time series. (j)– (l): Percentile of the TWS peak among the values surrounding the change years detected in (g)–(i).

## 3. Results and discussion

### 3.1. Water storage temporal variability

According to the seasonal Mann-Kendall and Theil-Sen slope results, the three studied GRACE solutions (CSR, GSFC, and JPL) present different behaviors in terms of long-term trend directions and magnitudes (Fig. 2a, b, and c). According to CSR, Region 3 and 4 experienced spatially predominant rising trends in TWS (Fig. 2a). The wetting trend over the southern regions appeared to be more prominent and statistically significant compared to Region 1. In the latter, the positive slopes are mostly found in areas near the Atlantic coastline, particularly in the far northeast of the country. The drying rates, on the other hand, were observed in some parts of Region 2, but mainly in the far western side of Region 1 with fewer isolated cases that were statistically significant at the 0.05 level. Contrasted observations can be drawn using the GSFC solution (Fig. 2b). While the upward trends were spatially limited in the west of Region 1 and east of Region 3, the depletion patterns were widespread all over the country. The trends were statistically significant in

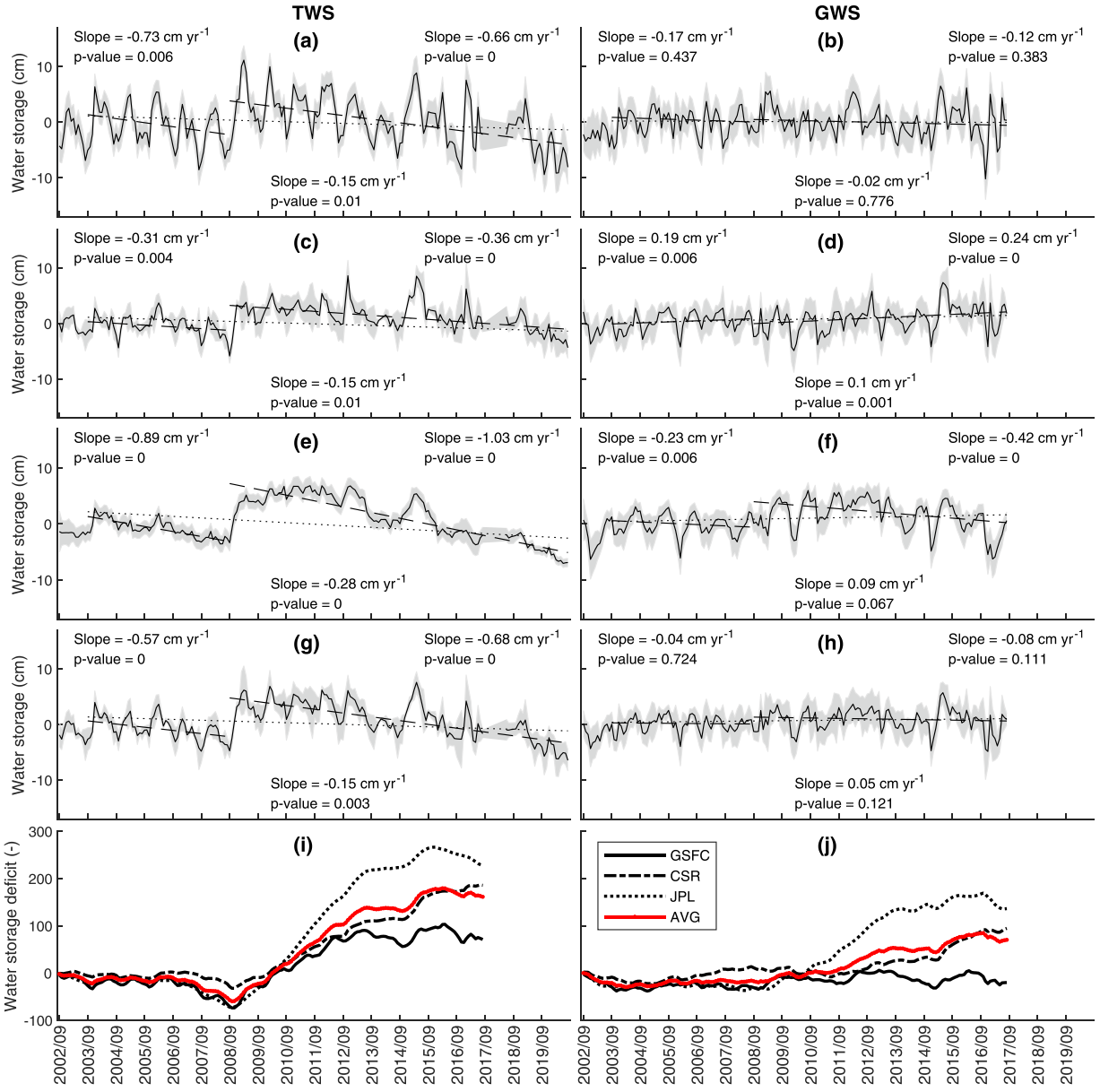


**Fig. 3.** Changes in GRACE-based TWS and GWS estimates over OER-TEN along with the associated errors (gray-shaded area). (a), (c), (e), and (g): Times series showing the fluctuations in TWS derived from GRACE GSFC, CSR, JPL, and AVG mascon solutions. (b), (d), (f), and (h) same as in (a), (c), (e), and (g), but for the GWS. (i) and (j): cumulative water storage as computed using the standardized groundwater index for TWS (i) and GWS (j). We note that the GWS reference period was limited to 09/2002 – 08/2017 due to the availability of SM data.

the majority of cases (Region 3 and Region 4), but particularly strong in Region 2. The TWS trends from JPL show roughly similar patterns as those depicted by GSFC, but with less spatial details. Statistically significant decreasing tendencies were found in the majority of Region 2, in the south of Region 4, and with relatively higher rates in the eastern part of Region 1. Increasing slopes were widespread in Region 3 and of less extent in Region 1, mostly of small amplitudes. Regional and global trend maps are often used to assess the long-term tendencies and emphasize the underlying factors of wetting and drying conditions over large scales (Hasan, 2019; Milewski et al., 2020; Rodell et al., 2018; Tapley et al., 2019). However, sometimes these tendencies can be unreal and temporarily caused by natural patterns or remarkable wetting events (Ahmed et al., 2021; Rodell et al., 2018; Sharma et al., 2016). Consequently, one could falsely draw conclusions that do not describe the real situation and give confidence about the sustainability of the groundwater when it is actually in depletion. Numerous authors reported that the presence of significant breaks in time series can strongly influence the long-term trend lines by causing slope dampening and signs reversal (Militino et al., 2020; Sharma et al., 2016). Given that, we investigated the presence of change points in TWS over Morocco (Fig. 2g, h, and i). Multiple change points were detected in $TWS_{CSR}$ (six), $TWS_{GSFC}$ (five), and $TWS_{JPL}$ (six) anomalies (Fig. 2g, h, and i). The temporal position of the change points differs depending on solutions and regions. The ones detected in CSR showed a certain spatial variability, with five different years were found in Region 1 (2008, 2009, 2010, 2014, and 2015), three in Region 2 (2009, 2014, and 2015) and Region 3 (2009, 2014, and 2015), and two (2007 and 2008) in Region 4. In the GSFC, they seemed relatively spatially consistent as two main change points were widespread, 2008 detected in Region 1 and 2012 in Region 2, 3, and 4, in addition to three others (2006, 2010, and 2014) scattered in small areas. According to JPL, four change years were detected in Region 1 (2008, 2009, 2010, and 2015), two in Region 2 (2009 and 2015) and Region 3 (2007 and 2015), and three in Region 4 (2006, 2007, and 2010). Moreover, the TWS peaks near the detected change points are generally among the highest over the full study period, except in Region 4 for CSR and GSFC. They correspond to percentiles between 82 and 100, which may indicate that the data have witnessed a sharp break in the mean and slope, possibly provoked by a potential recharge event.

For further inspection, we analyzed the temporal variation of the $TWS_{CSR}$, $TWS_{GSFC}$, $TWS_{JPL}$, $TWS_{AVG}$, and their respective GWS estimates over the OER-TEN (Fig. 3a-h). Each of the TWS and GWS time series was tested for trend and three trend lines were reported on each of the subplots. The first line, in dots, represents the overall trend of the water storage considering the whole study period (09/2002–08/2020). The other two lines represent the tendency before and after 2008/2009, detected as a significant change point in TWS of all solutions (Fig. 2). The full-time series of the TWS and GWS show completely different trends, depending on solutions. While the TWS (Fig. 3a, c, e, and g) demonstrates a significant decreasing tendency for all four TWS time series with rates of $-0.15 \pm 0.07$ cm $yr^{-1}$ (CSR), $-0.15 \pm 0.11$ cm $yr^{-1}$ (GSFC), $-0.28 \pm 0.11$ cm $yr^{-1}$ (JPL), and $-0.15 \pm 0.09$ cm $yr^{-1}$ (AVG), the GWS (Fig. 3b, d, f, and h) appeared to be increasing or near-steady over the studied period. The rising tendency was statistically significant only for $GWS_{CSR}$ ($+0.1 \pm 0.05$ cm $yr^{-1}$). However, blindly interpreting the trend slope values can be misleading, particularly for the GWS given its inconsistency with the decline in GWL records reported in several studies (Ahmed et al., 2021; Hssaisoune et al., 2020; Ouassanouan et al., 2022; Rafik et al., 2021). Thus, neither the positive trends nor those seeming near-steady should be directly considered as indicators of gaining in water storage or sustainability of the water table. Different factors can be the source of the tendency appearing as positive. Firstly, the inadequacy of the soil moisture data, with overly estimated magnitudes, can cause exaggerated subtraction of water quantities from the TWS. This can lead to GWS time series with unrealistic temporal patterns. Secondly, trend rates were necessarily influenced by the significant change in the mean of the GWS after 2008 that could have a role in stretching the trend lines upwards resulting in apparent wetting patterns. Overall, the different solutions seemed to be wetter in the second half of the study period than in the first one. Except for GSFC which exhibited a small drying slope, the cumulative water storage deficit consistently increased in 2008 onwards due to the frequent occurrence of above-normal months (Fig. 3i and j). As we split the reference period at the change point, we note that the GWS from most solutions was actually declining during the two sub-periods (2002–2007 and 2008–2020).

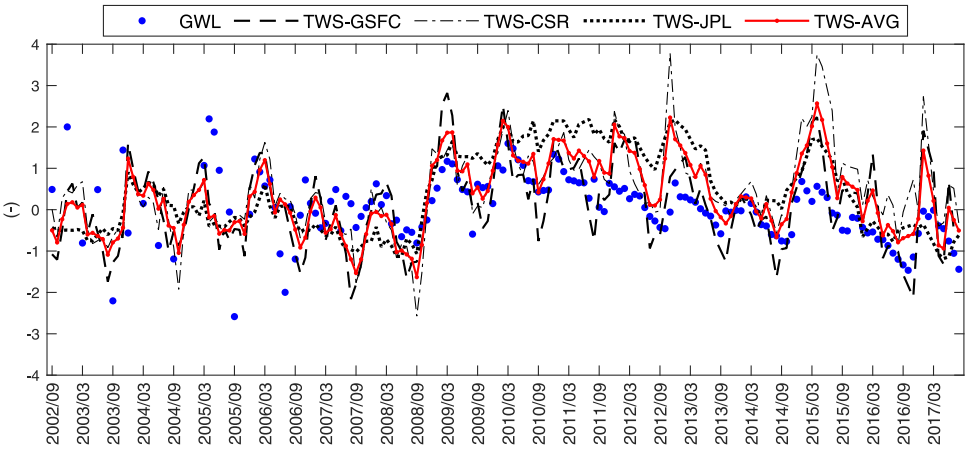


**Fig. 4.** Standardized time series of the GWL, $TWS_{GSFC}$, $TWS_{CSR}$, $TWS_{JPL}$, and $TWS_{AVG}$. The discontinuities in the GWL before 2007 are due to missing data.

Overall, since 2002, the study region underwent a significant depletion according to all TWS time series. This depletion could have been stronger if it was not for the sudden rise in the TWS that concurred with the change point in 2008/2009. The latter consists of a potential recharge event of the groundwater storage, which is clearly captured by the piezometer observations (Fig. 4). Following the same approach as for the GWS, we note that the terrestrial water reservoirs were subject to intermittent depletion episodes of relatively stronger magnitudes. During the 2002–2008 period, a statistically significant decrease was observed for $TWS_{CSR}$ ($-0.31 \pm 0.22$ cm $yr^{-1}$), $TWS_{GSFC}$ ($-0.73 \pm 0.29$ cm $yr^{-1}$), $TWS_{JPL}$ ($-0.89 \pm 0.2$ cm $yr^{-1}$), and $TWS_{AVG}$ ($-0.57 \pm 0.22$ cm $yr^{-1}$) that was ruptured thanks to the potential recharge event. If the declining tendency continued at the same rate, the TWS peak in 2008/2009 would have been $-1.39 \pm 2.37$ cm (CSR), $-2.63 \pm 4.18$ cm (GSFC), $-3.57 \pm 3.85$ cm (JPL), and $-2.48 \pm 3.03$ cm (AVG) instead of 3.27 cm, 11.17 cm, 4.14 cm, and 6.19 cm, respectively. However, even with the water levels being temporarily remedied, the depletion resumed as strong as it was before the breakpoint. The median decreasing rates of the second period (after 2008/2009) were also statistically significant, with the magnitudes obtained by the JPL ($-1.03 \pm 0.11$) solution being greater than those obtained based on the CSR ($-0.31 \pm 0.1$ cm $yr^{-1}$), GSFC ($-0.66 \pm 0.14$ cm $yr^{-1}$), and AVG ($-0.68 \pm 0.1$ cm $yr^{-1}$) solutions.

### 3.2. GRACE versus groundwater level

As demonstrated earlier, different inferences can be drawn about the temporal variation of the TWS and GWS as we use different GRACE solutions. Thus, the use of one solution over the other, or even the average of various solutions, should be done with care to avoid misleading conclusions. Nevertheless, there is a necessity for GRACE evaluation against the in-situ records to appropriately select the data that best match the temporal patterns of the GWL. In this section, we examined the relationship between the standardized GWL and three GRACE mascon solutions (CSR, GSFC, and JPL), in addition to their ensemble mean time series (AVG, Fig. 4), employing the SCC and RMSE metrics. It should be noted that because of the abundance of missing data, particularly between 2002 and 2006, the analysis was done in two parts. We used the full-time series (2002/2017) in the first one, while in the second one only the segment with the most consistent data (2007/2017) was considered. We note that the GRACE solutions performed differently with reference to the GWL (Table 1). Overall, the TWS time series provided by the GSFC and AVG seemed to better capture the GWL temporal patterns compared to those provided by the CSR and JPL. According to SCC and RMSE indicators, $TWS_{AVG}$ showed better agreement to the GWL changes with an overall SCC (RMSE) of 0.61 (0.88), followed by $TWS_{GSFC}$ with 0.58 (0.89). Furthermore, the relationship between the two data sources was stronger in the second part of the time series with the preeminence of $TWS_{AVG}$ (SCC=0.79 and RMSE=0.79) and $TWS_{GSFC}$ (SCC=0.71 and RMSE=0.77) over the rest of the solutions. The correlation coefficients obtained here lay within the same range as what was reported in several regions over the world (Bhanja et al., 2016; Hasan, 2019; Xie et al., 2018). This highlights GRACE's significance for groundwater monitoring and modeling. However, one should be careful when choosing the GRACE solution and soil moisture data to be used for the water balance equation resolution. Our findings suggest that in some cases, the TWS can match the GWL fluctuations well better than the GWS (it exhibited greater correlation coefficients and lower RMSEs by an average of 0.2–0.5 and 0.1–0.3 points, respectively). This can be partly attributed, as mentioned earlier, to the inadequacy of the model-based soil moisture estimates for the studied context. Previous studies employed soil moisture from the Global Land Data Assimilation System (GLDAS) model and found GWS tendencies that were similar to what was reported here for SURFEX (Ahmed et al., 2021; Milewski et al., 2020).

### 3.3. GRACE, SCA, and rainfall interaction

To emphasize the interaction between surface water intakes and TWS anomalies we investigated the changes in rainfall and SCA. We observe that the peaks captured by GRACE in 2008/2009 and 2014/2015 correspond to remarkably wet conditions (Fig. 5a). 130 mm $yr^{-1}$ and 95 mm $yr^{-1}$ above the long-term rainfall average were registered in 2008/2009 and 2014/2015, respectively. Both years were among the wettest all over the reference period, as they belong to the 10th decile. 2008/2009 ($P_{rank}$=97) was the second most wet year on record, since the 1970 s, and 2014/2015 was the fourth with a $P_{rank}$ of 92. Their precedence was widespread over most of the study region, particularly 2008/2009. According to the PERSIANN-CDR product (Fig. 5b), the same year occupied ranks from the 65th to the 96th, being above the 80th (90th) rank over 75% (25%) of OER-TEN. The ranking of 2014/2015, on the other hand, was less spatially prominent with $P_{rank}$ values below 85 at 75% of the grid-cells. Additionally, Fig. 6 shows that during the same

**Table 1**
The SCC and RMSE computed between the GRACE-based estimates and the standardized GWL.

| | SCC | | RMSE | |
|---|---|---|---|---|
| | 2002/2017 | 2007/2017 | 2002/2017 | 2007/2017 |
| TWS GSFC | 0.58 | 0.71 | 0.89 | 0.77 |
| TWS CSR | 0.5 | 0.65 | 1.11 | 1.10 |
| TWS JPL | 0.54 | 0.75 | 1.04 | 0.99 |
| TWS AVG | 0.61 | 0.79 | 0.88 | 0.79 |
| GWS GSFC | 0.4 | 0.5 | 1.04 | 0.93 |
| GWS CSR | -0.08 | -0.01 | 1.41 | 1.37 |
| GWS JPL | 0.19 | 0.36 | 1.25 | 1.18 |
| GWS AVG | 0.24 | 0.39 | 1.06 | 0.95 |

years, the mountainous region received the snow for longer periods and over larger extents. In almost 50% of the snowy season, the elevations above 1000 m a.s.l. were covered at 9–68% and 10–53% in 2008/2009 and 2014/2015, respectively. Notably, 2008/2009 ($Q_{75}$=22%) had more snow days of large extents than any other year including 2014/2015 ($Q_{75}$=17%).

Similar patterns can be deduced when analyzing the three rainfall indices (NWD, NCWD, and MCWD) calculated using daily measurements with six different thresholds for wet day definition (Fig. 7a-c). We note that the two TWS peaks can be associated with the number of wet days and, the frequency and length of the wet spells. The peaks seemed to take place under a large number of wet days, especially when they occur consecutively. The corresponding years can be clearly distinguished among the period 2002–2015, particularly 2008/2009. This holds true for most rainfall thresholds, but with a larger extent at 1 mm $d^{-1}$. Under this threshold, 80 (19) and 60 (15) wet days (CWD) were recorded in 2008/2009 and 2014/2015, respectively. The maximum length of the wet spells was 7 (2008/2009) and 9 (2014/2015) consecutive days, with median lengths of 3 days in 2008/2009 and 2 days in 2014/2015.

The above-mentioned observations may indicate that precipitation can be a potential contributor to the relative enhancement of terrestrial water storage over the OER-TEN. This is in line with the findings of isotopic studies that examined the interaction between surface and groundwater in Oum Er-Rbia and Tensift river basins (Bouchaou et al., 2009; Bouimouass et al., 2020; N'da et al., 2016). The authors agreed on the major role that rainfall and snowmelt play in recharging the underlying aquifers. However, one may wonder about the nature of this contribution. Is it related to the total amount of water produced by rainfall and snowmelt for a certain period or to the daily temporal distribution of these totals?

For further investigation, the relationship of the TWS time series versus SCA metrics and rainfall indices were graphically interpreted (Fig. 8a) and statistically explored based on the Spearman correlation coefficient (Fig. 8b and c). Only the $TWS_{AVG}$ and $TWS_{GSFC}$ were considered here, given their better agreement with the GWL observations compared to the $TWS_{JPL}$, $TWS_{CSR}$, $GWS_{GSFC}$, $GWS_{JPL}$, and $GWS_{CSR}$ estimates. The $TWS_{AVG}$ and $TWS_{GSFC}$ exhibited a clear seasonality over the studied period (Fig. 8a). They took lower values in the late summer and maximum values frequently occurred in the late winter and early spring. Generally, the TWS peaks seemed to be shifted compared to the observed peaks in precipitation. This suggests that the rise in TWS in the spring can be a kind of response to precipitation feeding the terrestrial water reservoirs during the wet period (November–April). This observation is further supported by the correlation coefficients reported in Fig. 8b and c. The results show that the TWS poorly correlates with the raw SCA and rainfall total data. For zero-month lag, the SCCs from $TWS_{AVG}$ ($TWS_{GSFC}$) were on average 0.55 (0.4) for SCA metrics and 0.33 (0.26) for the total rainfall. The correlation became stronger as the time lag is increased to reach a maximum at a specific value depending on variables. The three snow metrics (Max, Avg, and Med SCA) agreed on a maximum correlation at 1 month of lag, with a

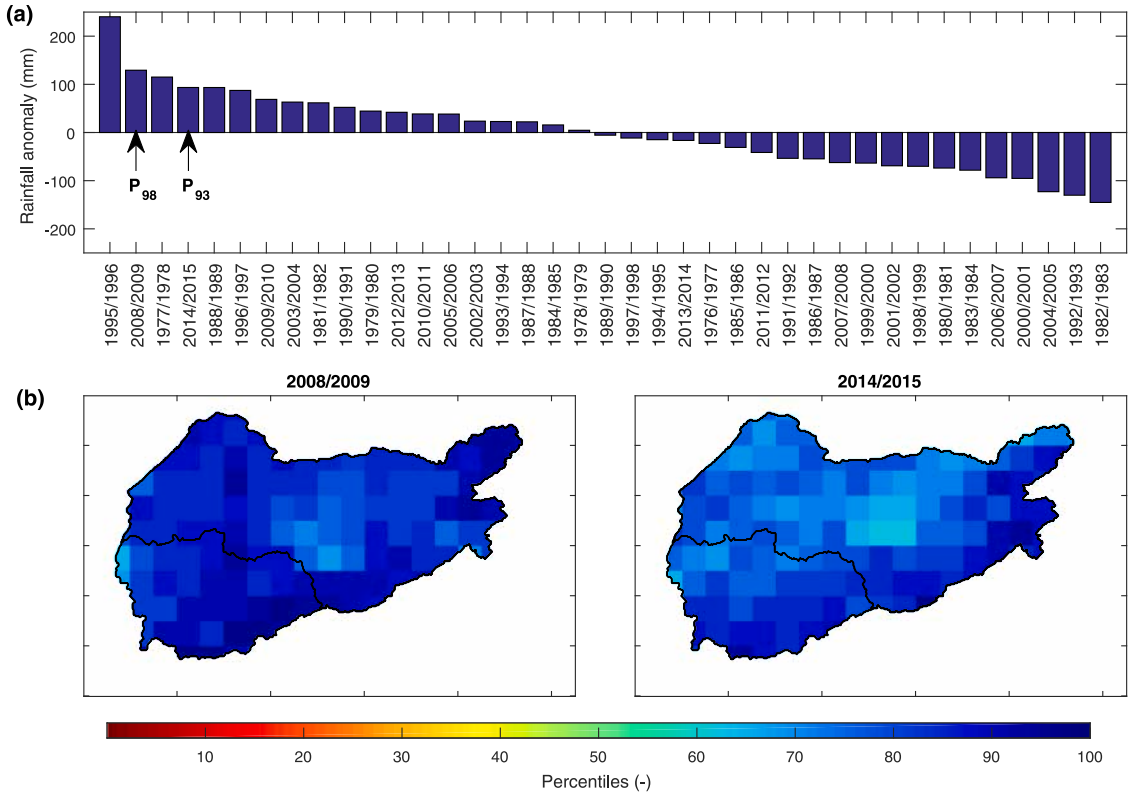


**Fig. 5.** Percentiles of the annual rainfall totals. (a): Annual rainfall anomalies calculated using rain gauge observations. The two arrows in (a), indicate the position and percentiles ($P_{rank}$) of the 2008/2009 and 2014/2015 years. (b): The spatial distribution of annual rainfall percentiles corresponding to the two aforementioned years. The percentiles in (b) were derived based on PERSIANN-CDR gridded rainfall data annual estimates.

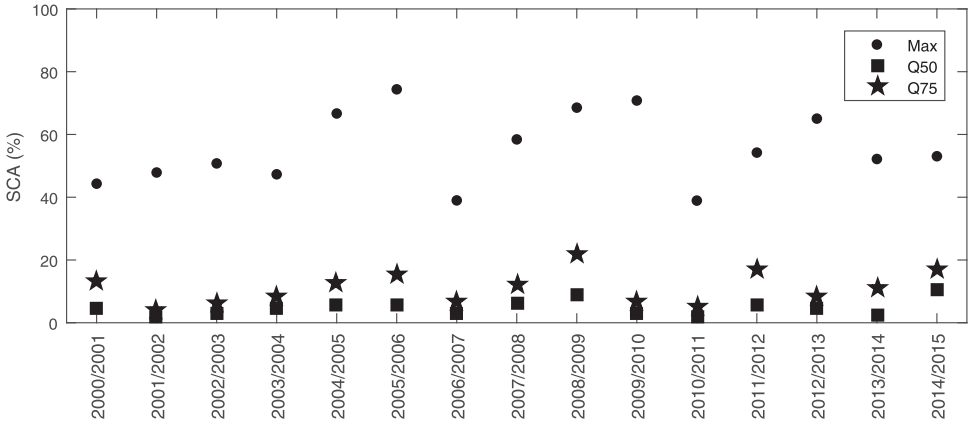


**Fig. 6.** Annual changes in SCA Percentage relative to the OER-TEN's mountainous region. Max, Q75, and Q50 refer to the SCA percentage corresponding to the maximum, 75th quartile, and 50th quantile, respectively.

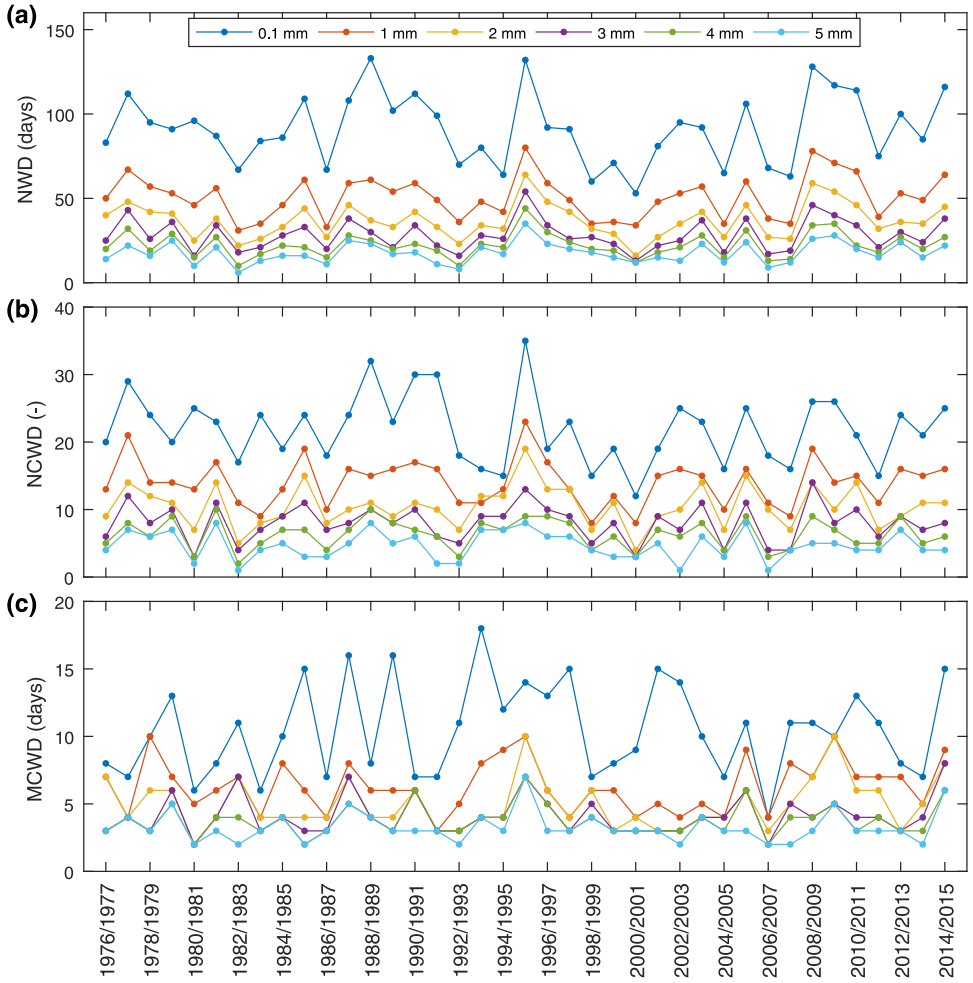


**Fig. 7.** Annual changes in rainfall daily indices. (a): The number of wet days (NWD). (b): The number of consecutive wet days (NCWD, more than 2 wet days in a row). (c): The maximum length of consecutive wet days (MCWD). The rainfall indices were retrieved using six different rainfall thresholds (0.1 mm, 1 mm, 2 mm, 3 mm, 4 mm, and 5 mm) to define a day as wet.

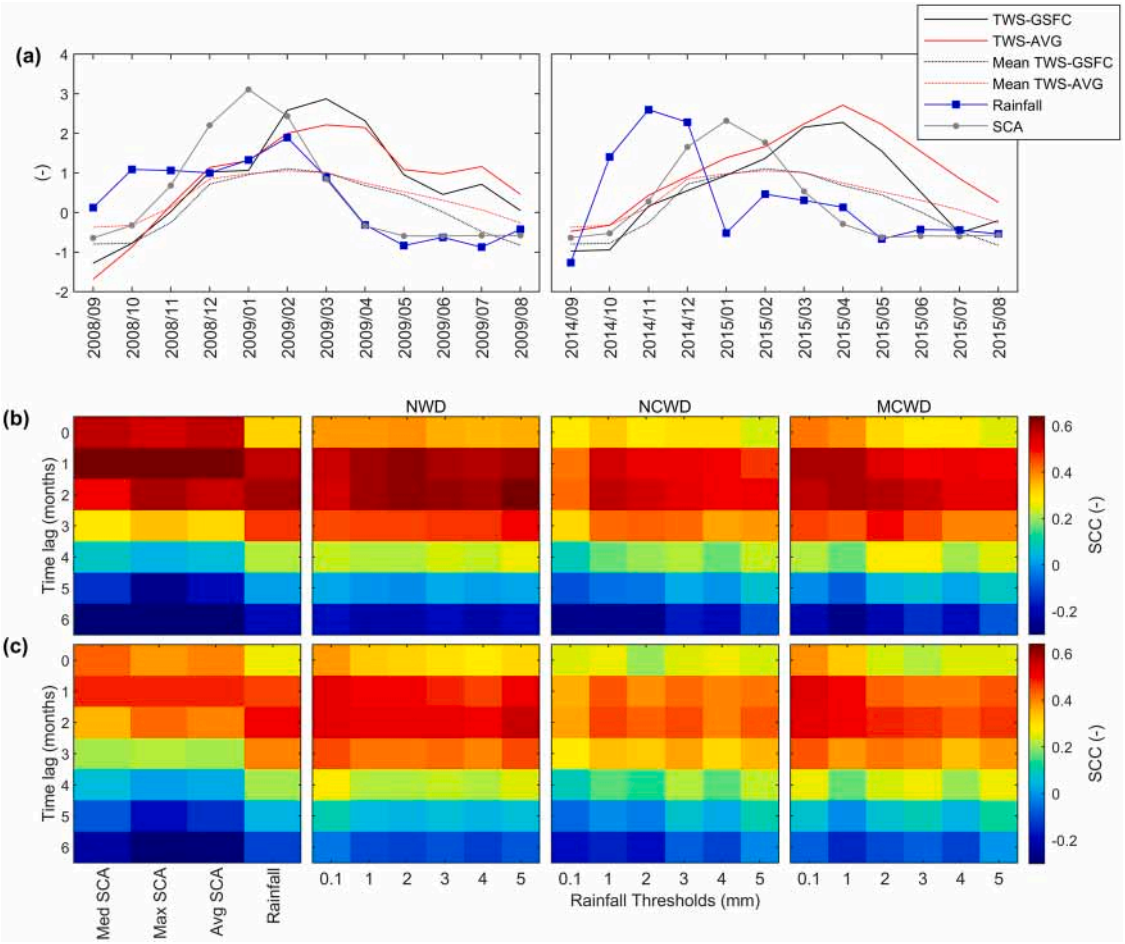


**Fig. 8.** The interaction between $TWS_{GSFC}$ and $TWS_{AVG}$, and climate variables. (a): The interannual mean of $TWS_{GSFC}$ and $TWS_{AVG}$ in addition to the SCA, Total rainfall, $TWS_{GSFC}$, and $TWS_{AVG}$ standardized monthly time series for 2008/2009 (left) and 2014/2015 (right). (b): Spearman correlation coefficients between $TWS_{GSFC}$ and monthly time series of SCA metrics (Med: median, Max: Maximum, and Avg: Average) and rainfall indices calculated for the period 2002–2015. (c): same as in (b) but for the $TWS_{AVG}$. The Spearman correlation was calculated by lagging the SCA metrics and rainfall indices by 0–6 months relative to $TWS_{GSFC}$ and $TWS_{AVG}$.

slight precedence of the Avg SCA and Max SCA over the Med SCA. The lag can be relatively higher when the snow cover is abundant. The TWS peaks during 2008/2009 and 2014/2015, for instance, respectively occurred in March and April (Fig. 8a). They were about two to three months behind the snow peak (January) and generally dephased by one to two months compared to the peak (February) of the TWS interannual average. The monthly rainfall, on the other hand, showed the highest agreement with the $TWS_{AVG}$ and $TWS_{GSFC}$ after 1–2 months of lag. Similar phase shifts were found for rainfall in tropical and subtropical African regions (Ahmed et al., 2011; Humphrey et al., 2016). The reported shifts were explained by the decay in water mass storage primarily caused by delayed water movements within the soil profile (Ahmed et al., 2011). The average and total rainfall have been widely used to study the interaction between surface water intakes and GRACE monthly patterns (Ahmed et al., 2021, 2011; Asoka et al., 2017; Humphrey et al., 2016; Rodell et al., 2018; Xie et al., 2018). Either by trendline comparison or correlation analysis, aggregated rainfall was found to significantly modulate the terrestrial water storage (Asoka et al., 2017; Humphrey et al., 2016; Xie et al., 2018). Here, we found that the indices describing the rainfall distribution have a relatively stronger relationship with the TWS time series compared to the monthly totals. This was mainly true for the NWD and MCWD as they respectively exhibited correlation coefficients around 0.62 (0.53) and 0.59 (0.54). Our results suggest that the frequency of wet days and the length of the wet spells can have more to say in the replenishment process of aquifers than the total and average monthly rainfall. This can be explained by the fact that abundant wet days assure continuous water supply to the soil, mainly when they occur consecutively. This also can allow less activation of the evapotranspiration process (given the shortage of direct solar energy), which can give more chance for the infiltrated water to percolate deeper and amply contribute to the groundwater flow.

## 4. Conclusions

In this study, we examined the terrestrial water variation as provided by the GRACE gravity anomalies over Morocco. Three mascon solutions (JPL, CSR, and GSFC) and their ensemble average (AVG) were analyzed using change point and trend tests. Additionally, Spearman correlation coefficient and Root Mean Square Error were employed to assess the GRACE estimates' correspondence with the GWL. Moreover, the analysis of GRACE data with climate variables was conducted to understand how the temporal changes in SCA and rainfall can explain the terrestrial water monthly patterns, considering multiple time lags.

The trend analysis, conducted using the seasonal Mann-Kendall test and Sen Slope estimator, revealed different terrestrial water tendencies. There was a spatial predominance of depletion patterns followed by small magnitude wetting slopes. However, the presence of significant change points within the time series seemed to have relatively masked the actual situation. In the northern region, for instance, the significant breakpoint identified in 2008, which corresponds to a remarkable natural groundwater recharge event, relatively caused a dampening of the overall depletion rate. The long-term trend slopes were relatively weaker (between $-0.28 \pm 0.11$ cm $yr^{-1}$ and $-0.15 \pm 0.07$ cm $yr^{-1}$) compared to those calculated when the time series were split at the change point. Our analysis focused on OER-TEN showed that the declining rates (between $-1.03 \pm 0.11$ cm $yr^{-1}$ and $-0.31 \pm 0.1$ cm $yr^{-1}$) were relatively stronger before and after the change point. This suggests that, since 2002, the region underwent intermittent depletion episodes interrupted by a temporary rise of the water table fed by surface water. Generally, the terrestrial water storage patterns were found to be linked with the changes in SCA and Rainfall. Our results indicated that the $TWS_{AVG}$ and $TWS_{GSFC}$, the best to describe the GWL temporal patterns, showed the highest correlations with the SCA metrics and rainfall indices after 1 – 3 months of lag. In particular, the number of wet days and the length of consecutive wet days exhibited relatively better correlations compared to the monthly totals. These findings suggest that, in addition to the SCA and total rainfall, more interest should be given to the rainfall distribution when studying the underlying sources of the groundwater natural recharge.

## CRediT authorship contribution statement

**Hamza Ouatiki**: Conceptualization, Formal analysis, Software, Methodology, Writing – original draft, Writing – review & editing. **Abdelghani Boudhar**: Conceptualization, Methodology, Funding acquisition, Writing – review & editing. **Marc Leblanc**: Conceptualization, Methodology, Funding acquisition, Writing – review & editing. **Younes Fakir**: Writing – review & editing. **Abdelghani Chehbouni**: Conceptualization, Methodology, Funding acquisition, Writing – review & editing.

## Declaration of Competing Interest

The authors declare that they have no known competing financial interests or personal relationships that could have appeared to influence the work reported in this paper.

## Data availability

Data will be made available on request.

## Acknowledgments

This study was supported by the "MorSnow-1" research program within the International Water Research Institute (IWRI), Mohammed VI Polytechnic University (UM6P), Morocco (Accord spécifique n° 39 entre OCP S.A et UM6P), the "African Geospatial Data Portal Frameworks For Science, Capacity-Building And Decision-Making Purposes" project within the Center for Remote Sensing Applications (CRSA-UM6P), Morocco (Accord spécifique n° 89 entre OCP S.A et UM6P), and by the Continental Surfaces and Interfaces in the Mediterranean Area (SICMED) program. The authors acknowledge the availability of GRACE and MODIS data from the contributor space agencies and in situ observations from Oum Er-Rbia and Tensift hydraulic agencies. We would also like to thank Clément Albergel and Météo-France for providing SURFEX soil moisture data.

## References

Ahmed, M., 2020. Sustainable management scenarios for northern Africa's fossil aquifer systems. J. Hydrol. 589, 125196 https://doi.org/10.1016/j.jhydrol.2020.125196.

Ahmed, M., Aqnouy, M., Stitou El Messari, J., 2021. Sustainability of Morocco's groundwater resources in response to natural and anthropogenic forces. J. Hydrol. 603 https://doi.org/10.1016/j.jhydrol.2021.126866.

Ahmed, M., Sultan, M., Wahr, J., Yan, E., 2014. The use of GRACE data to monitor natural and anthropogenic induced variations in water availability across Africa. Earth-Sci. Rev. 136, 289–300. https://doi.org/10.1016/j.earscirev.2014.05.009.

Ahmed, M., Sultan, M., Wahr, J., Yan, E., Milewski, A., Sauck, W., Becker, R., Welton, B., 2011. Integration of GRACE (Gravity Recovery and Climate Experiment) data with traditional data sets for a better understanding of the timedependent water partitioning in African watersheds. Geology 39, 479–482. https://doi.org/10.1130/G31812.1.

Ahmed, M., Wiese, D.N., 2019. Short-term trends in Africa's freshwater resources: rates and drivers. Sci. Total Environ. 695, 133843 https://doi.org/10.1016/j.scitotenv.2019.133843.

Albergel, C., Dutra, E., Bonan, B., Zheng, Y., Munier, S., Balsamo, G., de Rosnay, P., Muñoz-Sabater, J., Calvet, J.C., 2019. Monitoring and forecasting the impact of the 2018 summer heatwave on vegetation. Remote Sens. 11, 1–22. https://doi.org/10.3390/rs11050520.

Albergel, C., Munier, S., Jennifer Leroux, D., Dewaele, H., Fairbairn, D., Lavinia Barbu, A., Gelati, E., Dorigo, W., Faroux, S., Meurey, C., Le Moigne, P., Decharme, B., Mahfouf, J.F., Calvet, J.C., 2017. Sequential assimilation of satellite-derived vegetation and soil moisture products using SURFEX-v8.0: LDAS-Monde assessment over the Euro-Mediterranean area. Geosci. Model Dev. 10, 3889–3912. https://doi.org/10.5194/gmd-10-3889-2017.

Ashouri, H., Hsu, K.L., Sorooshian, S., Braithwaite, D.K., Knapp, K.R., Cecil, L.D., Nelson, B.R., Prat, O.P., 2015. PERSIANN-CDR: daily precipitation climate data record from multisatellite observations for hydrological and climate studies. Bull. Am. Meteorol. Soc. 96, 69–83. https://doi.org/10.1175/BAMS-D-13-00068.1.

Asoka, A., Gleeson, T., Wada, Y., Mishra, V., 2017. Relative contribution of monsoon precipitation and pumping to changes in groundwater storage in India. Nat. Geosci. 10, 109–117. https://doi.org/10.1038/ngeo2869.

Bahir, M., Ouhamdouch, S., Ouazar, D., 2021. An assessment of the changes in the behavior of the groundwater resources in arid environment with global warming in Morocco. Groundw. Sustain. Dev. 12, 100541 https://doi.org/10.1016/j.gsd.2020.100541.

Behrangi, A., Gardner, A., Reager, J.T., Fisher, J.B., Yang, D., Huffman, G.J., Adler, R.F., 2018. Using GRACE to estitmate snowfall accumulation and assess gauge undercatch corrections in high latitudes. J. Clim. 31, 8689–8704. https://doi.org/10.1175/JCLI-D-18-0163.1.

Bhanja, S.N., Mukherjee, A., Saha, D., Velicogna, I., Famiglietti, J.S., 2016. Validation of GRACE based groundwater storage anomaly using in-situ groundwater level measurements in India. J. Hydrol. 543, 729–738. https://doi.org/10.1016/j.jhydrol.2016.10.042.

Bhanja, S.N., Zhang, X., Wang, J., 2018. Estimating long-term groundwater storage and its controlling factors in Alberta, Canada. Hydrol. Earth Syst. Sci. 22, 6241–6255. https://doi.org/10.5194/hess-22-6241-2018.

Bloomfield, J.P., Marchant, B.P., 2013. Analysis of groundwater drought building on the standardised precipitation index approach. Hydrol. Earth Syst. Sci. 17, 4769–4787. https://doi.org/10.5194/hess-17-4769-2013.

Bouchaou, L., Michelot, J.L., Qurtobi, M., Zine, N., Gaye, C.B., Aggarwal, P.K., Marah, H., Zerouali, A., Taleb, H., Vengosh, A., 2009. Origin and residence time of groundwater in the Tadla basin (Morocco) using multiple isotopic and geochemical tools. J. Hydrol. 379, 323–338. https://doi.org/10.1016/j.jhydrol.2009.10.019.

Boudhar, A., Boulet, G., Hanich, L., Sicart, J.E., Chehbouni, A., 2016. Energy fluxes and melt rate of a seasonal snow cover in the Moroccan High Atlas. Hydrol. Sci. J. 61, 931–943. https://doi.org/10.1080/02626667.2014.965173.

Boudhar, A., Duchemin, B., Hanich, L., Boulet, G., abdelghan, 2011. Spatial distribution of the air temperature in mountainous areas using satellite thermal infra-red data. C. R. Geosci. 343 https://doi.org/10.1016/j.crte.2010.11.004.

Boudhar, A., Ouatiki, H., Bouamri, H., Lebrini, Y., Karaoui, I., Hssaisoune, M., Arioua, A., Benabdelouahab, T., 2020. Hydrological response to snow cover changes using remote sensing over the Oum Er Rbia Upstream Basin, Morocco. In: Rebai, N., Mastere, M. (Eds.), Mapping and Spatial Analysis of Socio-Economic and Environmental Indicators for Sustainable Development. Springer, Cham, Cham, Switzerland, pp. 95–102. https://doi.org/10.1007/978-3-030-21166-0_9.

Bouimouass, H., Fakir, Y., Tweed, S., Leblanc, M., 2020. Groundwater recharge sources in semiarid irrigated mountain fronts. Hydrol. Process. 34, 1598–1615. https://doi.org/10.1002/hyp.13685.

Döll, Petra, Schmied, Hannes Müller, Schuh, Carina, Portmann, Felix, Eicker T., Annette, 2014. Global-scale assessment of groundwater depletion and related groundwater abstractions: combining hydrological modeling with information from well observations and GRACE satellites. Water Resources Research 50, 5698–5720. https://doi.org/10.1002/2014WR015595.

Doumbia, C., Castellazzi, P., Rousseau, A.N., Amaya, M., 2020. High resolution mapping of ice mass loss in the Gulf of Alaska from constrained forward modeling of GRACE data. Front. Earth Sci. 7 https://doi.org/10.3389/feart.2019.00360.

Eicker, A., Jensen, L., Wöhnke, V., Dobslaw, H., Kvas, A., Mayer-Gürr, T., Dill, R., 2020. Daily GRACE satellite data evaluate short-term hydro-meteorological fluxes from global atmospheric reanalyses. Sci. Rep. 10, 1–10. https://doi.org/10.1038/s41598-020-61166-0.

Entekhabi, B.D., Njoku, E.G., Neill, P.E.O., Kellogg, K.H., Crow, W.T., Edelstein, W.N., Entin, J.K., Goodman, S.D., Jackson, T.J., Johnson, J., Kimball, J., Piepmeier, J. R., Koster, R.D., Martin, N., Mcdonald, K.C., Moghaddam, M., Moran, S., Reichle, R., Shi, J.C., Spencer, M.W., Thurman, S.W., Tsang, L., Zyl, J.Van, 2010. The Soil Moisture Active Passive (SMAP). IEEE Proc. 98, 704–716.

Fakir, Y., Bouimouass, H., Constantz, J., 2021. Seasonality in intermittent streamflow losses beneath a semiarid Mediterranean Wadi. Water Resour. Res. 57 https://doi.org/10.1029/2021WR029743.

Ferreira, V.G., Yong, B., Tourian, M.J., Ndehedehe, C.E., Shen, Z., Seitz, K., Dannouf, R., 2020. Characterization of the hydro-geological regime of Yangtze River basin using remotely-sensed and modeled products. Sci. Total Environ. 718, 137354 https://doi.org/10.1016/j.scitotenv.2020.137354.

Filahi, S., Tanarhte, M., Mouhir, L., Morhit, M., El, Tramblay, Y., 2015. Trends in indices of daily temperature and precipitations extremes in Morocco. Theor. Appl. Climatol. 124, 959–972. https://doi.org/10.1007/s00704-015-1472-4.

Filahi, S., Tramblay, Y., Mouhir, L., Diaconescu, E.P., 2017. Projected changes in temperature and precipitation indices in Morocco from high-resolution regional climate models. Int. J. Climatol. 37, 4846–4863. https://doi.org/10.1002/joc.5127.

Gleason, C.J., Wada, Y., Wang, J., 2018. A hybrid of optical remote sensing and hydrological modeling improves water balance estimation. J. Adv. Model. Earth Syst. 10, 2–17. https://doi.org/10.1002/2017MS000986.

Hadri, A., Saidi, M.E.M., Boudhar, A., 2021. Multiscale drought monitoring and comparison using remote sensing in a Mediterranean arid region: a case study from west-central Morocco. Arab. J. Geosci. 14 https://doi.org/10.1007/s12517-021-06493-w.

Hall, D.K., Riggs, G.A., 2016. MODIS/Terra Snow Cover Daily L3 Global 500m SIN Grid, Version 6. [h17v5]. Boulder, Colorado USA. NASA National Snow and Ice Data Center Distributed Active Archive Center. https://doi.org/https://doi.org/10.5067/MODIS/MOD10A1.006. [2018–02-04].

Hasan, E., 2019. Assessment of Physical Water Scarcity in Africa Using GRACE and TRMM Satellite Data. https://doi.org/10.3390/rs11080904.

Hasan, E., Tarhule, A., Hong, Y., Moore III, B., 2019. Assessment of physical water scarcity in Africa using GRACE and TRMM satellite data. Remote Sens. 11, 1–17. https://doi.org/10.3390/rs11080904.

Hssaisoune, M., Bouchaou, L., Sifeddine, A., Bouimetarhan, I., Chehbouni, A., 2020. Moroccan groundwater resources and evolution with global climate changes. Geosciences 10, 1–26. https://doi.org/10.3390/geosciences10020081.

Humphrey, V., Gudmundsson, L., Seneviratne, S.I., 2016. Assessing global water storage variability from GRACE: trends, seasonal cycle, subseasonal anomalies and extremes. Surv. Geophys. 37, 357–395. https://doi.org/10.1007/s10712-016-9367-1.

IPCC, 2014. Climate change 2014 synthesis report. Geneva, Switzerland.

Jin, S., Zhang, T.Y., Zou, F., 2017. Glacial density and GIA in Alaska estimated from ICESat, GPS and GRACE measurements. J. Geophys. Res. Earth Surf. 122, 76–90. https://doi.org/10.1002/2016JF003926.

Kendall, M.G., 1938. A new measure of rank correlation. Biometrika 30, 81–93. https://doi.org/10.2307/2332226.

Killick, R., Fearnhead, P., Eckley, I.A., 2012. Optimal detection of changepoints with a linear computational cost. J. Am. Stat. Assoc. 107, 1590–1598. https://doi.org/10.1080/01621459.2012.737745.

Knippertz, P., Christoph, M., Speth, P., 2003. Long-term precipitation variability in Morocco and the link to the large-scale circulation in recent and future climates. Meteorol. Atmos. Phys. 83, 67–88. https://doi.org/10.1007/s00703-002-0561-y.

Landerer, F.W., Cooley, S.S., 2021. GRACE-FO Level-3 Data Product User Handbook. California.

Lavielle, M., 2005. Using penalized contrasts for the change-point problem. Signal Process. 85, 1501–1510. https://doi.org/10.1016/j.sigpro.2005.01.012.

Leblanc, M.J., Tregoning, P., Ramillien, G., Tweed, S.O., Fakes, A., 2009. Basin-scale, integrated observations of the early 21st century multiyear drought in Southeast Australia. Water Resour. Res. 45, 1–10. https://doi.org/10.1029/2008WR007333.

Leblanc, M., Tweed, S., Ramillien, G., Tregoning, P., Frappart, F., Fakes, A., Cartwright, I., 2011. Groundwater change in the Murray basin from long- term in- situ monitoring and GRACE estimates. In: Climate Change Effects on Groundwater Resources: A Global Synthesis of Findings and Recommendations, pp. 169–187.

Luthcke, S.B., Sabaka, T.J., Loomis, B.D., Arendt, A.A., McCarthy, J.J., Camp, J., 2013. Antarctica, Greenland and Gulf of Alaska land-ice evolution from an iterated GRACE global mascon solution. J. Glaciol. 59, 613–631. https://doi.org/10.3189/2013JoG12J147.

Mann, H.B., 1945. Nonparametric tests against trend. Econometrica 13, 245–259. https://doi.org/10.2307/1907187.

Marchane, A., Boudhar, A., Wassim Baba, M., Hanich, L., Chehbouni, A., 2021. Snow lapse rate changes in the Atlas Mountain in Morocco based on MODIS time series during the period 2000–2016. Remote Sens. 13, 3370.

Marchane, A., Jarlan, L., Hanich, L., Boudhar, A., Gascoin, S., Tavernier, A., Filali, N., Le Page, M., Hagolle, O., Berjamy, B., 2015. Assessment of daily MODIS snow cover products to monitor snow cover dynamics over the Moroccan Atlas mountain range. Remote Sens. Environ. 160, 72–86. https://doi.org/10.1016/j.rse.2015.01.002.

Mehrnegar, N., Jones, O., Singer, M.B., Schumacher, M., Bates, P., Forootan, E., 2020. Comparing global hydrological models and combining them with GRACE by dynamic model data averaging (DMDA). Adv. Water Resour. 138 https://doi.org/10.1016/j.advwatres.2020.103528.

Milewski, A., Seyoum, W.M., Elkadiri, R., Durham, M., 2020. Multi-scale hydrologic sensitivity to climatic and anthropogenic changes in Northern Morocco. Geosciences 10, 1–22. https://doi.org/10.3390/geosciences10010013.

Militino, A.F., Moradi, M., Ugarte, M.D., 2020. On the performances of trend and change-point detection methods for remote sensing data. Remote Sens. 12, 1–25. https://doi.org/10.3390/rs12061008.

Neves, M.C., Nunes, L.M., Monteiro, J.P., 2020. Evaluation of GRACE data for water resource management in Iberia: a case study of groundwater storage monitoring in the Algarve region. J. Hydrol. Reg. Stud. 32 https://doi.org/10.1016/j.ejrh.2020.100734.

Niu, G.Y., Seo, K.W., Yang, Z.L., Wilson, C., Su, H., Chen, J., Rodell, M., 2007. Retrieving snow mass from GRACE terrestrial water storage change with a land surface model. Geophys. Res. Lett. 34, 1–5. https://doi.org/10.1029/2007GL030413.

N'da, A.B., Bouchaou, L., Reichert, B., Hanich, L., Ait Brahim, Y., Chehbouni, A., Beraaouz, E.H., Michelot, J.L., 2016. Isotopic signatures for the assessment of snow water resources in the Moroccan high Atlas mountains: contribution to surface and groundwater recharge. Environ. Earth Sci. 75 https://doi.org/10.1007/s12665-016-5566-9.

Oki, T., Sud, Y.C., 1998. Design of Total Runoff Integrating Pathways (TRIP)—a global river channel network. Earth Interact. 2, 1–36. https://doi.org/10.1175/1087-3562(1998)002<0001:dotrip>2.3.co;2.

Ouassanouan, Y., Fakir, Y., Simonneaux, V., Kharrou, M.H., Bouimouass, H., Najar, I., Benrhanem, M., Sguir, F., Chehbouni, A., 2022. Multi-decadal analysis of water resources and agricultural change in a Mediterranean semiarid irrigated piedmont under water scarcity and human interaction. Sci. Total Environ. 834, 155328 https://doi.org/10.1016/j.scitotenv.2022.155328.

Ouatiki, H., Boudhar, A., Ouhinou, A., Arioua, A., Hssaisoune, M., Bouamri, H., Benabdelouahab, T., 2019. Trend analysis of rainfall and drought over the Oum Er-Rbia River Basin in Morocco during 1970–2010. Arab. J. Geosci. 12, 1–11. https://doi.org/10.1007/s12517-019-4300-9.

Ouatiki, H., Boudhar, A., Ouhinou, A., Beljadid, A., Leblanc, M., Chehbouni, A., 2020. Sensitivity and interdependency analysis of the HBV conceptual model parameters in a semi-arid. Water 12, 2440. https://doi.org/10.3390/w12092440.

Ouatiki, H., Boudhar, A., Chehbouni, A., 2022. Remote sensing datasets' capability to reproduce the observed rainfall patterns over semi-arid watersheds. Atmos. Res. In review.

Peterson, T.C., Folland, C.C., Gruza, G., Hogg, W., Mokssit, A., Plummer, N., 2001. Report on the activities of the Working Group on Climate Change Detection and Related Rapporteurs 1998–2001, Rep. WCDMP-47, WMO-TD 1071.

Rafik, A., Bahir, M., Beljadid, A., Ouazar, D., Chehbouni, A., Dhiba, D., Ouhamdouch, S., 2021. Surface and groundwater characteristics within a semi-arid environment using hydrochemical and remote sensing techniques. Water 13. https://doi.org/10.3390/w13030277.

Rodell, M., Famiglietti, J.S., Wiese, D.N., Reager, J.T., Beaudoing, H.K., Landerer, F.W., Lo, M.H., 2018. Emerging trends in global freshwater availability. Nat. Anal. 557, 651–659. https://doi.org/10.1038/s41586-018-0123-1.

Sadeghi, M., Gao, L., Ebtehaj, A., Wigneron, J.P., Crow, W.T., Reager, J.T., Warrick, A.W., 2020. Retrieving global surface soil moisture from GRACE satellite gravity data. J. Hydrol. https://doi.org/10.1016/j.jhydrol.2020.124717.

Sen, P.K., 1968. Estimates of the regression coefficient based on Kendall'S Tau. J. Am. Stat. Assoc. 63, 1379–1389. https://doi.org/10.1080/01621459.1968.10480934.

Sharma, S., Swayne, D.A., Obimbo, C., 2016. Trend analysis and change point techniques: a survey. Energy Ecol. Environ. 1, 123–130. https://doi.org/10.1007/s40974-016-0011-1.

Shen, H., Leblanc, M., Frappart, F., Seoane, L., Grady, D.O., Olioso, A., Tweed, S., 2017. A comparative study of GRACE with continental evapotranspiration estimates in Australian semi-arid and arid basins: sensitivity to climate variability and extremes. Water 7, 1–19. https://doi.org/10.3390/w9090614.

Shen, H., Leblanc, M., Tweed, S., Liu, W., 2015. Groundwater depletion in the Hai River Basin, China, from in situ and GRACE observations. Hydrol. Sci. J. 60, 671–687. https://doi.org/10.1080/02626667.2014.916406.

Tapley, B.D., Bettadpur, S., Watkins, M., Reigber, C., 2004. The gravity recovery and climate experiment: mission overview and early results. Geophys. Res. Lett. 31, 1–4. https://doi.org/10.1029/2004GL019920.

Tapley, B.D., Watkins, M.M., Flechtner, F., Reigber, C., Bettadpur, S., Rodell, M., Sasgen, I., Famiglietti, J.S., Landerer, F.W., Chambers, D.P., Reager, J.T., Gardner, A. S., Save, H., Ivins, E.R., Swenson, S.C., Boening, C., Dahle, C., Wiese, D.N., Dobslaw, H., Tamisiea, M.E., Velicogna, I., 2019. Contributions of GRACE to understanding climate change. Nat. Clim. Chang. 9, 358–369. https://doi.org/10.1038/s41558-019-0456-2.

Theil, H., 1950. A rank-invariant method of linear and polynomial regression analysis. I, II, III. Ned. Akad. Van. Wet. Proc. 53, 386–392. , 521–525, 1397–1412.

Watkins, M.M., Wiese, D.N., Yuan, D.-N., Boening, C., Landerer, F.W., 2015. Improved methods for observing Earth's time variable mass distribution with GRACE using spherical cap mascons. J. Geophys. Res. Solid Earth 120, 2648–2671. https://doi.org/10.1002/2014JB011547.

Xiao, Ruya, He, Xiufeng, Zhang, Yonglei, Ferreira, Vagner, Chang G., Liang, 2015. Monitoring groundwater variations from satellite gravimetry and hydrological models: a comparison with in-situ measurements in the mid-atlantic region of the United States. Remote Sensing 7 (1), 686–703. https://doi.org/10.3390/rs70100686.

Xie, X., Xu, C., Wen, Y., Li, W., 2018. Monitoring groundwater storage changes in the Loess Plateau using GRACE satellite gravity data, hydrological models and coal mining data. Remote Sens. 10, 1–18. https://doi.org/10.3390/rs10040605.

Zhao, M., Geruo, A., Velicogna, I., Kimball, J.S., 2017. Satellite observations of regional drought severity in the continental United States using GRACE-based terrestrial water storage changes. J. Clim. 30, 6297–6308. https://doi.org/10.1175/JCLI-D-16-0458.1.